Deletion of the *GPIdeAc* Gene Alters the Location and Fate of Glycosylphosphatidylinositol Precursors in *Trypanosoma brucei*†

M. Lucia S. Güther, Alan R. Prescott, and Michael A. J. Ferguson*

Division of Biological Chemistry and Molecular Microbiology, The Wellcome Trust Biocentre, The School of Life Sciences, University of Dundee, Dundee DD1 5EH, Scotland, U.K.

Received May 23, 2003; Revised Manuscript Received September 1, 2003

ABSTRACT: Glycosylphosphatidylinositol (GPI) membrane anchors are ubiquitous among the eukaryotes. In most organisms, the pathway of GPI biosynthesis involves inositol acylation and inositol deacylation as discrete steps at the beginning and end of the pathway, respectively. The bloodstream form of the protozoan parasite *Trypanosoma brucei* is unusual in that these reactions occur on multiple GPI intermediates and that it can express side chains of up to six galactose residues on its mature GPI anchors. An inositol deacylase gene, *T. brucei GPIdeAc*, has been identified. A null mutant was created and shown to be capable of expressing normal mature GPI anchors on its variant surface glycoprotein. Here, we show that the null mutant synthesizes galactosylated forms of the mature GPI precursor, glycolipid A, at an accelerated rate (2.8-fold compared to wild type). These free GPIs accumulate at the cell surface as metabolic end products. Using continuous and pulse−chase labeling experiments, we show that there are two pools of glycolipid A. Only one pool is competent for transfer to nascent variant surface glycoprotein and represents 38% of glycolipid A in wild-type cells. This pool rises to 75% of glycolipid A in the *GPIdeAc* null mutant. We present a model for the pathway of GPI biosynthesis in *T. brucei* that helps to explain the complex phenotype of the *GPIdeAc* null mutant.

Many eukaryotic cell surface glycoproteins are attached to the plasma membrane by covalent linkage to a glycosylphosphatidylinositol (GPI)[1] anchor. The structure and biosynthesis of GPI membrane anchors and related molecules have been reviewed (*1*−*5*). The basic GPI core structure attached to protein is composed of $NH_2CH_2CH_2PO_4$H-6Manα1−2Manα1−6Manα1−4GlcNα1−6-D-*myo*-inositol-1-HPO_4-lipid (Et*N*P-Man_3GlcN-PI). This minimal GPI structure may contain different lipids and be embellished with additional ethanolamine phosphate groups and/or carbohydrate side chains in a species- and tissue-specific manner (*5*). For example, the mature GPI anchor attached to the variant surface glycoprotein (VSG) of *Trypanosoma brucei* has the structure Et*N*P-6(±Galα1−2)Manα1−2(±Gal*β*1−3)Manα1−6[±Galα1−2Galα1−6(±Galα1−2)Galα1−3]-Manα1−4GlcNα1−6-D-*myo*-inositol-1-HPO_4-*sn*-1,2-dimyristoylglycerol (*6*, *7*).

Protozoa tend to express significantly higher densities of cell surface GPI-anchored proteins than do higher eukaryotes. In particular, *T. brucei*, the causative agent of African sleeping sickness, expresses a dense cell surface coat consisting of approximately 5×10^6 dimers of a GPI-anchored VSG, whose principal purpose is to protect the parasite from the alternative complement pathway of the host and, through antigenic variation, from specific immune responses (*8*). This parasite also expresses an essential GPI-anchored transferrin receptor (*9*, *10*). Thus, inhibitors able to arrest the formation or transfer of GPI to *T. brucei* VSG and transferrin receptor should prove to be useful in the development of antiparasitic agents. This notion has been genetically validated for the disease-causing bloodstream form of *T. brucei*, where disruptions of the *TbGPI10* or *TbGPI12* genes, encoding the third mannosyltransferase (MT-3) and GlcNAc-PI de-*N*-acetylase of GPI anchor biosynthesis, respectively, have been shown to be lethal for the parasite (*11*, *12*).

The sequence of events underlying GPI biosynthesis has been studied in *T. brucei* (*13*−*18*), *Trypanosoma cruzi* (*19*), *Toxoplasma gondii* (*20*), *Plasmodium falciparum* (*21*), *Leishmania* (*22*−*24*), *Saccharomyces cerevisiae* (*25*−*27*), *Cryptococcus neoformans* (*28*), and mammalian cells (*3*, *29*−*31*). In all cases, GPI biosynthesis involves the transfer of GlcNAc from UDP-GlcNAc to phosphatidylinositol (PI) to give GlcNAc-PI via an endoplasmic reticulum (ER) membrane-bound multiprotein complex (*32*). This step occurs on the cytoplasmic face of the ER, as does the second step of the pathway, the de-N-acetylation of GlcNAc-PI to GlcN-PI (*33*). Notable differences between the *T. brucei* and mammalian GPI biosynthetic pathways occur from GlcN-PI onward, including the timing of inositol acylation and deacylation (*17*, *31*, *34*), fatty acid remodeling of *T. brucei* GPI anchors (*20*, *35*), and substrate channeling between the de-*N*-acetylase and the first mannosyltransferase (MT-1) (*36*). Inositol acylation (the transfer of fatty acid to the 2-OH group of the D-*myo*-inositol residue) of GlcN-PI either precedes or

† This work was supported by a Wellcome Trust program grant.

* To whom correspondence should be addressed: phone, 44-1382-344219; fax, 44-1382-345764; e-mail, m.a.j.Ferguson@dundee.ac.uk.

[1] Abbreviations: AHM, 2,5-anhydromannitol; ER, endoplasmic reticulum; Gal-A, galactosylated metabolites of glycolipid A; GPI, glycosylphosphatidylinositol; HPTLC, high-performance thin-layer chromatography; MT, α-mannosyltransferase; VSG, variant surface glycoprotein.

10.1021/bi034869g CCC: $25.00
Published on Web 11/15/2003

follows the action of the first mannosyltransferase (MT-1), as in mammalian cells and *T. brucei*, respectively (*1*, *17*, *34*). This difference was exploited in the discovery of the first generation of specific substrates (*37*) and inhibitors (*38*) of the *T. brucei* GPI biosynthetic pathway in vitro.

The expression cloning of the mammalian *PIG-M* (*39*) and *PIG-B* (*40*) genes, encoding the first and third α-mannosyltransferases of GPI biosynthesis (MT-1 and MT-3), has allowed the identification of the yeast and *T. brucei* homologues (*39*, *41*). The predicted topology of these Dol-*P*-Man multispanning ER-resident proteins strongly suggests that their active sites face the lumen of the ER (*39*). The same is true for the three putative ethanolamine phosphate (EtN*P*) transferases predicted to transfer EtN*P* to all three αMan residues of the GPI core structure in mammalian cells (*42*−*44*), of which only one homologue (*PIG-O*) appears to exist in *T. brucei*. The transamidase complex, which replaces C-terminal GPI anchor signal peptides for the preassembled GPI anchor precursor, is another multiprotein complex that resides in the lumen of the ER (*45*, *46*). Thus, in building models of GPI biosynthesis, the ER lumenal/cytoplasmic orientations of enzyme active sites must be taken into account. Of equal importance, significant proportions (up to 65%) of several GPI intermediates are accessible to membrane-impermeable probes in sealed *T. brucei* microsomes (*47*). It appears, therefore, that there are flippases to allow the flip-flop of GPI intermediates between the lumenal and cytoplasmic faces of the ER.

Of the remaining enzymes of GPI biosynthesis, little is known about MT-2 other than it is dependent on Dol-*P*-Man and, therefore, likely to resemble MT-1 and MT-3 in topology. The mammalian and yeast inositol acyltransferase genes (*PIG-W* and *GWT1*, respectively) have recently been cloned (*48*, *49*), and the active site of the predicted multispanning membrane protein has been suggested to face the lumen of the ER (*48*). An obvious *T. brucei* homologue of these genes has not been found. In *T. brucei*, one GPI inositol deacylase (GPIdeAc) has been purified and cloned. This is a nonessential gene, and at least one other inositol deacylase is clearly present (*50*).

In this paper, we have studied the perturbation to normal GPI metabolism caused by *GPIdeAc* deletion, together with an analysis of the proportion of mature GPI precursor (glycolipid A) molecules that are competent for transfer to nascent VSG molecules in wild-type and mutant parasites. The results provide new insights into the arrangement of the pathway in *T. brucei*, and these have been incorporated into a revised model of the pathway.

EXPERIMENTAL PROCEDURES

Immunofluorescence Microscopy. Cells were air-dried onto coverlips and fixed with 4% paraformaldehyde in trypanosome dilution buffer, permeabilized with 1% NP40 in PBS, blocked with 10% fish skin gelatin, and immunolabeled with mouse anti-HA antibody and rabbit anti-BiP antibody. Finally, they were counterstained with Alexa488 conjugated anti-rabbit and Alexa594 anti-mouse secondary antibodies (Molecular Probes) and DAPI. Specimens, mounted in hydromount, were examined using a 100× NA 1.4 Plan-Apochromat objective and recorded on a Zeiss DeltaVision restoration microscope (Applied Precision, Inc.) equipped with a three-dimensional motorized stage and a Photometrics CH350 camera. Images were deconvolved, and each image is a projection of 20 optical sections taken at 0.2 μM intervals.

Continuous and Pulse−*Chase Labeling of Trypanosomes with [^{3}H]Man.* Wild-type and *GPIdeAc* knockout trypanosomes were grown in HMI-9 medium containing 2.5 μg/mL G418 in a 5% CO_2 incubator. Cells were washed, preincubated with 0.8 μg/mL tunicamycin at 37 °C, and labeled with [^{3}H]Man as described before (*51*). At each time point, duplicate aliquots (250 μL; 5×10^6 cells) were taken for lipid extraction and for VSG quantification (*17*).

Hypotonic Lysis and Processing of the Released GPI Glycans. Wild-type and *GPIdeAc* knockout trypanosomes were labeled with [^{3}H]Man for 70 min, as described above, and washed once with 22 mM sodium phosphate, pH 7.8, containing 5 mM KCl, 80 mM NaCl, 1 mM $MgSO_4$, and 20 mM glucose. The parasites (2×10^8 cells) were lysed by resuspending them in 200 μL of water containing 1 μg/mL leupeptin, 0.1 mM TLCK, and 2 μg/mL aprotinin. After centrifugation (16000*g*, 5 min) protein was precipitated from the supernatant by the addition of 3 volumes of ethanol and incubation at −20 °C for 16 h. The insoluble material, mainly sVSG, was removed by centrifugation (16000*g*, 20 min at 4 °C). The supernatant was freeze-dried and dephosphorylated with 100 μL of aqueous 48% HF for 48 h at 0 °C. The sample was freeze-dried again and deaminated, reduced, and desalted as decribed in ref *52*. Digestions with coffee bean α-galactosidase (CBAG) were as described in ref *53*.

High-Performance Thin-Layer Chromatography. Lipid extracts labeled with [^{3}H]Man were processed as described (*17*) and run on silica 60 HPTLC plates using the solvent system chloroform/methanol/1 M ammonium acetate/13 M ammonia/water (180:140:9:9:23 v/v). The [^{3}H]Man-labeled GPI glycans were run on silica gel 60 HPTLC plates (before and after CBAG digestion) using three sequential developments with 1-propanol/acetone/water (9:6:5 v/v), 1-propanol/acetone/water (5:4:1 v/v), and 1-propanol/acetone/water (9:6:5 v/v) (*53*). The HPTLC plates were exposed to a tritium screen (Bas-IP, Fuji) followed by analysis and quantification in a phosphorimager (FLA 2000, Fuji).

Extraction and Mass Spectrometric Analysis of Polar GPI. Wild-type and *GPIdeAc* knockout trypanosomes were grown to late log phase and harvested by centrifugation (800*g*, 10 min, 4 °C). The cells were washed in PBS, and the resulting cell pellets (5×10^8 cells) were resuspended in 150 μL of PBS and extracted overnight at 4 °C by the addition of 1 mL of chloroform/methanol (1:1 v/v). After sonication, the extracts were centrifuged, and the supernatants were adjusted to chloroform/methanol/water (8:4:3 v/v) to form a biphasic mixture. After centrifugation, the upper phase was recovered and the lower phase was extracted twice with an equal volume of the preequilibrated upper phase. The combined upper phases were back-washed four times with 1 mL of the preequilibrated lower phase and dried under a stream of nitrogen. The products were partitioned between butan-1-ol and water (500 μL of each). The upper butanol phase was recovered, and the lower aqueous phase was reextracted twice with 500 μL of the preequilibrated upper phase. The combined butanol phases were back-extracted three times with an equal voume of the preequilibrated lower phase to remove salts. The washed butanol phase, containing polar

GPIs, was dried and redissolved in 40 μL of propan-1-ol/acetic acid/water (3:1:6 v/v). Aliquots (2 μL) were used to load nanospray tips (Micromass type F) for electrospray mass spectrometry (ES-MS). Samples were analyzed in positive ion mode with tip and cone voltages of 0.8 kV and 30 V, respectively, using a Micromass Quattro Ultima triple quadruplole mass spectrometer and a Micromass Q-Tof2 orthogonal quadrupole-time of flight mass spectrometer (Micromass, Manchester, U.K.). The triple quadrupole machine was programmed to record parent ion spectra (parents of *m*/*z* 495) with a collision voltage of 40 V and a collision argon pressure of 3×10^{-3} Torr. The Q-Tof instrument was programmed to collect daughter ion spectra of selected ions with a collision voltage between 26 and 30 V, depending on the parent ion. All spectra were collected and processed with Micromass Masslynx software.

Quantification of Polar GPIs by GC-MS. Following ES-MS analysis, the remainder of the polar GPI extracts (90%) were mixed with 10 pmol of *scyllo*-inositol, dried, deacylated with 200 μL of 7 M ammonia in 25% propan-1-ol (16 h at room temperature), and dried again. The residue was dissolved in 15 μL of 0.3 M sodium acetate, pH 4.0, and deaminated with 10 μL of 1 M sodium nitrite (4 h at room temperature). The products were reduced by addition of 5 μL of 0.4 M boric acid, 25 μL of 2 M sodium hydroxide, and 10 μL of 1 M sodium borodeuteride (16 h at 4 °C) and then neutralized with 100 μL of 1 M acetic acid. The products were desalted by passage through 0.25 mL of Dowex AG50 X12(H^+), elution with 1.25 mL of water, drying, addition of 0.25 mL of 2% acetic acid in methanol, and drying (four times). The products were dissolved in 50 μL of water, transferred to reaction tubes, dried, subjected to methanolysis (50 μL of 0.5 M HCl in methanol, 90 °C, 4 h), neutralized with 10 μL of pyridine, and dried. The products were reacted with 15 μL of trimethylsilylating reagent for 30 min at room temperature, and aliquots of 1.5 μL were analyzed by GC-MS (*52*) using selected ion monitoring for [1-^{2}H]-2,5-anhydromannitol-TMS_4 (*m*/*z* 204, 217, and 273; 7.5−21.5 min) and *scyllo*-inoisitol-TMS_6 (*m*/*z* 305 and 318; 21.5−30 min). Relative response factors were determined empirically by taking standards of D-glucosamine and *scyllo*-inositol through the whole protocol.

RESULTS

GPIdeAc May Be Located in a Subcompartment of the Endoplasmic Reticulum. Immunostaining of the bloodstream form of *GPIdeAc* knockout *T. brucei* cells (Δ*GPIdeAc::HYG*/Δ*GPIdeAc::PAC*) (*50*) with antibodies to the HA-eptiope tag gave negligible staining whereas the same cells transformed to overexpress HA-tagged GPIdeAc (Δ*GPIdeAc::HYG*/Δ*GPIdeAc::PAC*/*GPIdeAc*−*HA*^{Ti}) (*50*) gave detectable reticular and perinuclear staining, reminiscent of the endoplasmic reticulum (ER) and clearly distinct from lysosomes, endosomes, or Golgi apparatus that are concentrated exclusively in the posterior part of the cell, between the nucleus and the flagellar pocket (*54*−*56*) (data not shown). Additional immunostaining experiments with antibodies to a cytosolic marker, trypanothione reductase, showed a completely different (uniform) intracellular pattern, and staining of the single mitochondrion with mitotracker revealed a thin structure that runs the length of the cell body in these slender bloodstream form of parasites (*57*) (data not shown). We therefore performed dual labeling studies with rabbit antibodies to the *T. brucei* ER marker BiP (*58*) and mouse anti-HA antibodies. The reticular and perinuclear staining of the ER with anti-BiP antibodies can be seen in the knockout and overexpressing cells (Figure 1C,D) whereas similar (but weaker) anti-HA staining can be seen in the GPIdeAc-HA overexpressing cells (Figure 1A) but not in the *GPIdeAc* knockout cells (Figure 1B). To our surprise, merging of these images revealed little colocalization of the two staining patterns in the GPIdeAc-HA overexpressing cells (Figure 1E). On the other hand, close inspection of the images suggests that anti-HA and anti-BiP staining appears to be contiguous, suggesting that GPIdeAc may occupy a subcompartment of the ER dedicated to GPI biosynthesis and devoid of other markers (see Discussion).

GPIdeAc Knockout Trypanosomes Accumulate Gal-A GPI Glycolipids as Metabolic End Products. We reported previously that *GPIdeAc* knockout trypanosomes labeled with [^{3}H]-Man accumulate labeled galactosylated glycolipid A (Gal-A) GPI species and that this accumulation could be reversed by the introduction of an ectopic copy of *GPIdeAc* (*50*). Here, in four separate continuous labeling time course experiments, we show that Gal-A species accumulate linearly with time in both wild-type (Figure 2A) and *GPIdeAc* knockout trypanosomes (Figure 2B) and that the rate of accumulation is 2.8-fold greater in the *GPIdeAc* knockout cells. This linear accumulation of labeled Gal-A species is consistent with them being metabolic end products and contrasts with the rapid labeling of glycolipid A and glycolipid C species to steady state, typical of metabolic intermediates (Figure 2).

Free GPI Glycolipids Are Transported to the Cell Surface. Hypotonic osmotic lysis of the bloodstream form of *T. brucei* parasites allows access of the enzyme GPI-PLC to cell surface VSG (*59*−*61*). This phenomenon is used to distinguish cell surface VSG, which is released as soluble form sVSG, from VSG located in the ER/Golgi apparatus, which remains membrane-bound by its GPI anchor (*62*, *63*). We reasoned that the same treatment would cleave free GPI glycolipids at the cell surface but not those resident in the ER.

Wild-type and *GPIdeAc* knockout trypanosomes were labeled for 70 min with [^{3}H]Man, washed, and subjected to osmotic shock by suspension in water. In both cases, microscopic analysis suggested that cell lysis was 100%. The lysates were centrifuged to remove membrane-bound material, and the supernatant was deproteinated by precipitation with ethanol to remove sVSG. The resulting supernatant was dried, dephosphorylated with ice-cold 48% aqueous HF, and subjected to nitrous acid deamination and $NaBH_4$ reduction (*52*). Thus, labeled GPI glycolipids located at the cell surface were converted to labeled neutral glycans terminating in 2,5-anydromannitol (AHM). Analysis of these fractions by HPTLC and fluorography revealed labeled glycans comigrating with Man_3AHM and with $Gal_{4-6}Man_3$AHM, as well as uncharacterized material that remained at the origin and non-GPI material (digestion with jack bean α-mannosidase did not affect these bands) that migrated near the front (Figure 3). The identity of the $Gal_{4-6}Man_3$AHM glycans was confirmed by coffee bean α-galactosidase digestion, which converted them to a mixture of Man_3AHM and Gal_2Man_3-

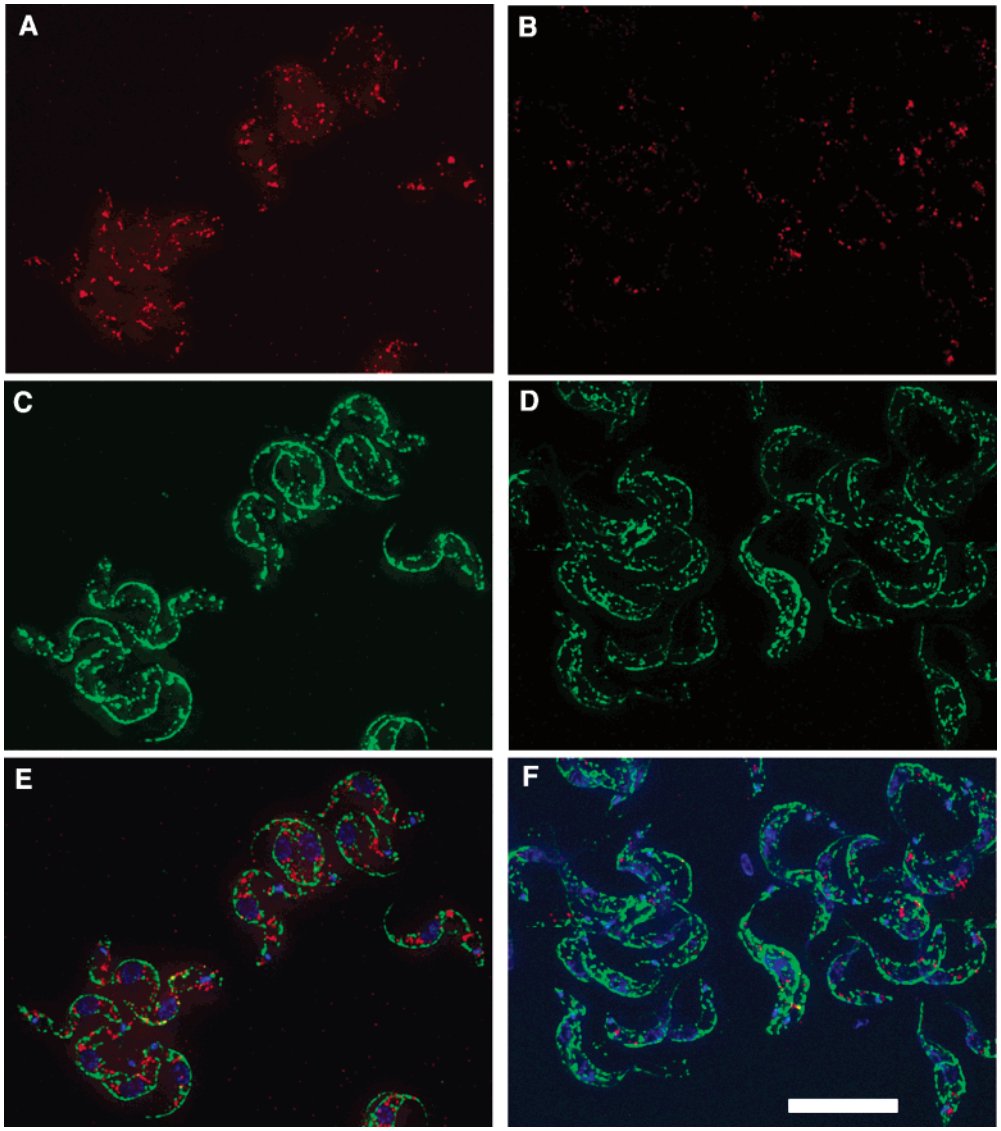

FIGURE 1: Immunolocalization of HA-tagged GPIdeAc expressed in *GPIdeAc* knockout bloodstream form trypanosomes. *GPIdeAc*$^{-/-}$ double knockout cells (B, D, and F) and *GPIdeAc*$^{-/-}$ double knockout cells expressing ectopic *GPIdeAc-HA* (A, C, and E) were stained with a mouse antibody to the HA tag (red channel, A and B) and a rabbit polyclonal antibody to the ER marker BiP (green channel, C and D). The merged images of both stains are shown in (E) and (F). The blue channel is DAPI staining for DNA that reveals the nucleus and the kinetoplast (mitochondrial DNA) that is adjacent to the flagellar pocket. The bar in (F) represents 10 μm.

AHM and Gal_1Man_3AHM,[2] as described in ref *7*. The patterns of labeled glycans isolated from wild-type and *GPIdeAc* knockout trypanosomes were quite similar but about 3-fold more intense in the knockout cells.

In summary, these data demonstrate (i) that Gal-A GPIs, and a small amount of glycolipid A, exit the ER and reach the cell surface in wild-type cells and (ii) that significantly more Gal-A GPIs and glycolipid A exit the ER and reach the cell surface in *GPIdeAc* knockout cells.

The Steady-State Levels of Gal-A Are Higher in GPIdeAc Knockout Trypanosome. The labeling experiments described above show that the rate of synthesis of Gal-A GPIs is greater in *GPIdeAc* knockout trypanosomes and that these molecules are transported to the cell surface. To examine the structures of the Gal-A species and to determine relative steady-state amounts of these molecules in wild-type and GPIdeAc knockout cells, polar GPIs were extracted and analyzed by mass spectrometry.

Both cell types were grown under identical conditions and harvested at the same phase of growth. Equivalent numbers of cells were extracted with chloroform/methanol/water, and polar GPI glycolipids [i.e., glycolipid A and Gal-A species but not glycolipid C (*64*)] were partitioned into the upper methanol/water-rich phase after the addition of water. This fraction was dried and partitioned between butan-1-ol and water. The butan-1-ol phase was back-washed with water and dried. These desalted fractions enriched in polar GPIs

[2] One of the Gal residues is βGal and therefore is resistant to coffee bean α-galactosidase, while one of the αGal residues is resistant to coffee bean α-galactosidase for steric reasons (*7*). Thus, starting from $Gal_{6-4}Man_3AHM$, i.e., ±Galα1−2Manα1−2(±Galβ1−3)Manα1−6(±Galα1−2Galα1−6(±Galα1−2)Galα1−3)Manα1−4AHM, the terminal coffee bean α-galactosidase digest will contain Gal_2Man_3AHM, Galα1−2Manα1−2(Galβ1−3)Manα1−6Manα1−4AHM, two glycoforms of Gal_1Man_3AHM, Galα1−2Manα1−2Manα1−6Manα1−4AHM and Man(Galβ1−3)Manα1−6Manα1−4AHM, and Man_3AHM, Manα1−2Manα1−6Manα1−4AHM.

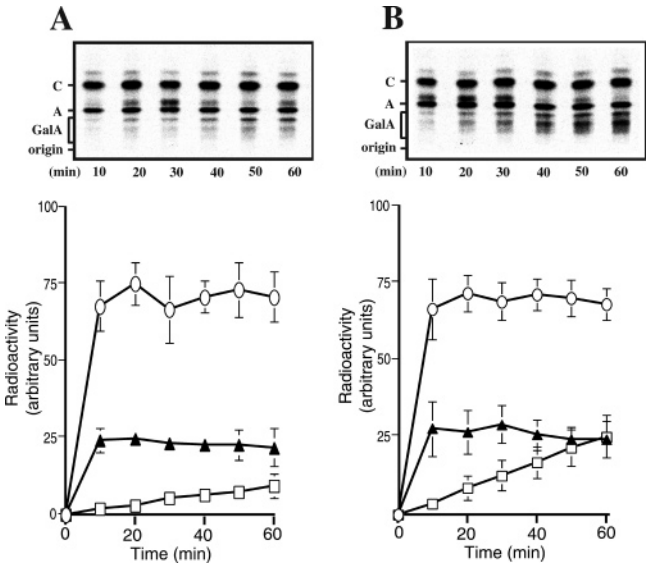

FIGURE 2: Continuous labeling of wild-type and *GPIdeAc* knockout trypanosomes with [^{3}H]Man. Wild-type (A) and *GPIdeAc* knockout (B) trypanosomes were metabolically labeled with [^{3}H]Man in four separate experiments. Aliquots of labeled cells were recovered at 10 min intervals, and total GPI glycolipids were extracted and analyzed by HPTLC and phosphorimagery. The upper panels show one representative radiochromatogram. The mean values of the phosphorimager signals (± 1 SD; $n = 4$) due to radioactivity in the glycolipid C (circles), glycolipid A (triangles), and Gal-A (squares) species are plotted as a function of time (lower panels).

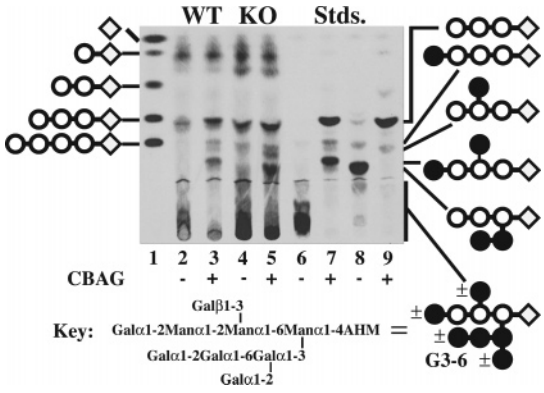

FIGURE 3: Analysis of metabolically radiolabeled GPI headgroups liberated by hypotonic lysis. Trypanosomes were labeled with [^{3}H]-Man for 70 min, washed, and subjected to hypotonic lysis. Released GPI headgroups were converted to neutral glycans, and those from wild-type (WT; lanes 2 and 3) and *GPIdeAc* knockout trypanosomes (KO; lanes 4 and 5) were analyzed by HPTLC and fluorography before (−) and after (+) digestion with coffee bean α-galactosidase (CBAG) alongside neutral glycan standards (lanes 1 and 6−9). The standards are a mixture of Man_{0-4}AHM (lane 1), $Gal_{3-6}Man_3$AHM (lanes 6 and 7), and Gal_2Man_3AHM (lanes 8 and 9).

were analyzed by positive ion electrospray mass spectrometry−mass spectrometry (ES-MS-MS) using a triple quadrupole mass spectrometer. Parent ion scanning mode was used (parents of *m*/*z* 495) to select for ions that contain dimyristoylglycerol (Figure 4A,B). In the *GPIdeAc* knockout trypanosome extract, the ions at *m*/*z* 763, 844, 926, 1006, 1087, 1168, and 1249 suggested the presence of $[M + 2H]^{2+}$ ions corresponding to glycolipid A [ethanolamine-*P*-Man_3-GlcN-(dimyristoyl)PI] and Gal-A GPI species containing 1−6 Gal residues, respectively (Figure 4B). These assignments were confirmed by ES-MS-MS daughter ion analysis of the aforementioned ions using a Q-Tof mass spectrometer (see Figure 4C for a representative spectrum). Analysis of the same fraction prepared from wild-type cells revealed a similar set of ions, but those due to Gal-A species were much less abundant (Figure 4A). In both samples, but particularly the wild-type sample, molecular species 12 Da larger (i.e., with doubly charged ion *m*/*z* values 6 units higher) were seen (Figure 4A,B). Daughter ion spectra of these ions revealed that they are formaldehyde Schiff base adducts of the Gal-A species with the Schiff base present exclusively on the (more reactive) ethanolamine group (Figure 4D). Presumably, one of the solvents used in the analysis contained a trace of formaldehyde, and the lower the concentration of GPI glycolipids, the higher the proportion of adducts.

To provide a more quantitative estimate of the polar GPI glycolipids, the fractions were mixed with an internal standard, O-deacylated, deaminated, and reduced to convert non-N-acetylated glucosamine to [1-^{2}H]-2,5-anhydromannitol. This GPI-specific derivative was analyzed as its TMS derivative by selected ion monitoring GC-MS. This is a very selective way of measuring GPI species and superior to *myo*-inositol analysis, which is prone to overestimation from contaminating inositol phospholipids (details to be published elsewhere). The results showed that there were 2.0 and 7.2 pmol of polar GPIs (glycolipid A + Gal-A) per 10^8 cells in the *GPIdeAc* knockout and wild-type trypanosome extracts, respectively. Thus, there are 3.6-fold more polar GPIs in the knockout cells.

The Accumulation of Gal-A in GPIdeAc Knockout Trypanosomes Correlates with an Increase in ER Lumenal Glycolipid A. The most likely explanation for the accumulation of Gal-A glycolipids in the knockout cells is a perturbation of the GPI biosynthetic pathway such that more glycolipid A is accessible to the relevant galactosyltransferases. It is known that glycolipid A can be found on both sides of the ER membrane (*47*), suggesting that there are at least two populations of glycolipid A: (a) that on the lumenal face of the ER that is competent for transfer to nascent VSG molecules and may be modified by ER-resident galactosyltransferases and (b) that on the cytoplasmic face of the ER that is incompetent for transfer to nascent VSG molecules and may not be modified by ER-resident galactosyltransferases. An increase in the amount of glycolipid A in the lumen of the ER would not alter GPI addition to nascent VSG [since VSG synthesis is rate-limiting (*65*, *66*)] but might reasonably be expected to give rise to more Gal-A species and to the exit of more free GPI glycolipids from the ER by mass action. There are two ways in which the proportion of glycolipid A in the lumen of the ER might be increased: (i) by increasing the total amount of glycolipid A and/or (ii) by altering the ratio of the cytoplasmic and lumenal forms of glycolipid A.

The data presented in Figure 2 suggested a modest (1.15-fold) increase in glycolipid A in *GPIdeAc* knockout trypanosomes compared with wild-type cells. Thus, the observed 2.8-fold increase in the rate of formation of Gal-A species is not simply due to an increase in total glycolipid A.

To test the possibility that the increase in Gal-A species was due to a significant increase in the proportion of glycolipid A in the lumen of the ER, we measured the proportion of glycolipid A that is competent for transfer to VSG polypeptide (a parameter that has not previously been

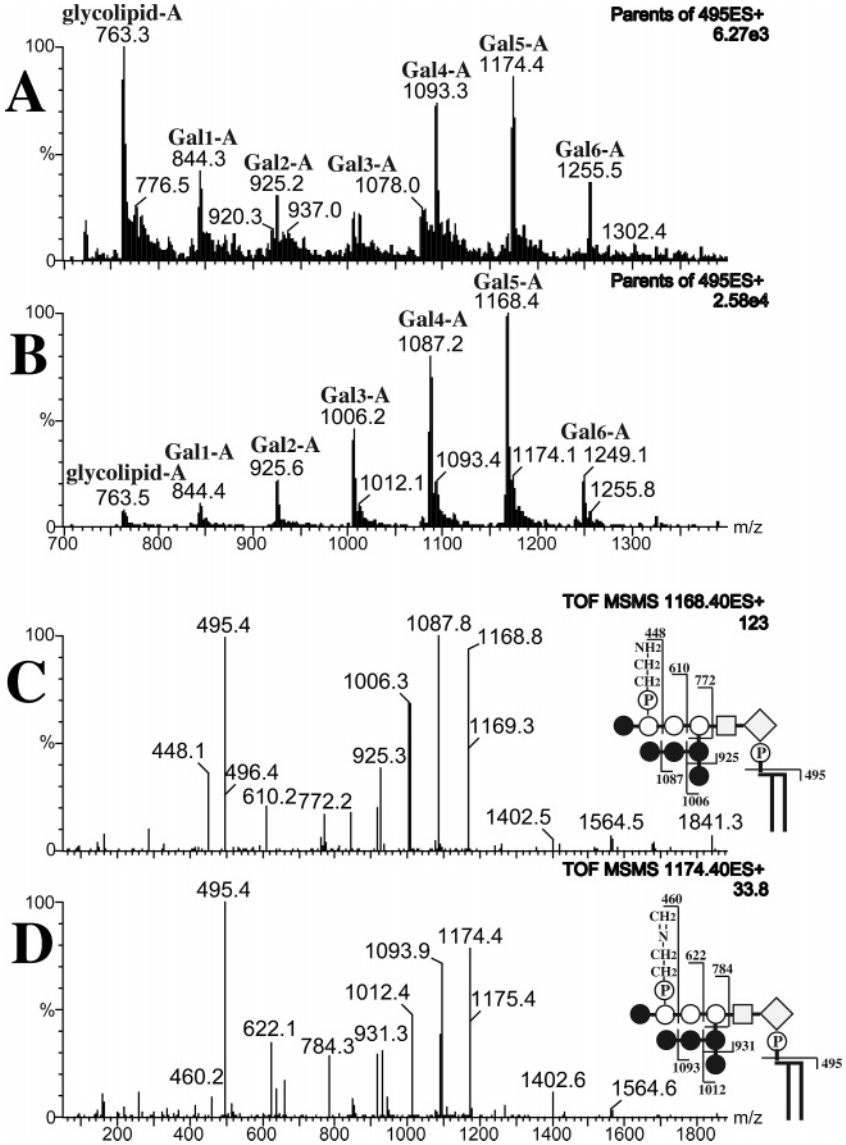

FIGURE 4: Mass spectrometric analysis of the polar GPIs extracted from wild-type and *GPIdeAc* knockout trypanosomes. Polar GPI extracts from wild-type (panel A) and *GPIdeAc* knockout trypanosomes (panel B) were analyzed for dimyristoylglycerol-containing GPI glycolipids by parent ion scanning (parents of *m*/*z* 495). Representative daughter ion spectra of the $[M + 2H]^{2+}$ parent ions at *m*/*z* 1168.4 from the *GPIdeAc* knockout sample (panel C) and *m*/*z* 1174.4 from the wild-type sample (panel D) show that these molecular species are identical apart from the Schiff base adduct present in *m*/*z* 1174.4, which can be located to the ethanolamine group by the *m*/*z* 460, 622, and 784 daughter ion series (see inset).

measured) in wild-type and *GPIdeAc* knockout trypanosomes.

Wild-type and *GPIdeAc* knockout trypanosomes were labeled with [^{3}H]Man in the presence of tunicamycin[3] with and without a mannose chase after 20 min. Samples were processed for VSG analysis by SDS−PAGE, fluorography, and scintillation counting of digested VSG bands and for glycolipid analysis by HPTLC and phosphorimager quantification. The experiments were performed twice, and radioactivities in glycolipid A and VSG-linked GPIs were normalized to the 20 min (0 min chase) values. In the wild-type cells, we observed the usual slow chase of radioactivity from the glycolipid A pool (*51*), such that between 20 and 40 min (0−20 min of chase) the amount of labeled glycolipid A present in the cells was 81 ± 6% of the no-chase control (Figure 5A). In this same period (20−40 min), the increase of GPI label into VSG was only 31 ± 6% of the no-chase control (Figure 5B). This discrepancy can be explained if only a portion (38 ± 12%) of the radiolabeled glycolipid A is available for transfer to VSG over the period of the chase. This figure agrees well with the estimate of 35% ER lumenal glycolipid A measured using PI-PLC and ConA probes and sealed microsomes (*47*). When the same experiment was performed with *GPIdeAc* knockout trypanosomes, the chase kinetics of glycolipid A were similar and the amount of labeled glycolipid A present in the cells was 80 ± 8% of the no-chase control (Figure 5C) whereas the rate of increase of GPI label into VSG was 60 ± 10% of the no-chase control (Figure 5D), suggesting that, in these cells, 75 ± 18% of glycolipid A was competent for transfer to VSG. This apparent doubling in the proportion of glycolipid A competent for transfer to VSG (and therefore in the lumen of

[3] Preincubation and labeling were performed with tunicamycin to inhibit protein N-glycosylation such that all [^{3}H]Man label associated with VSG is solely due to the incorporation of [^{3}H]Man-labeled glycolipid A into VSG (*17*).

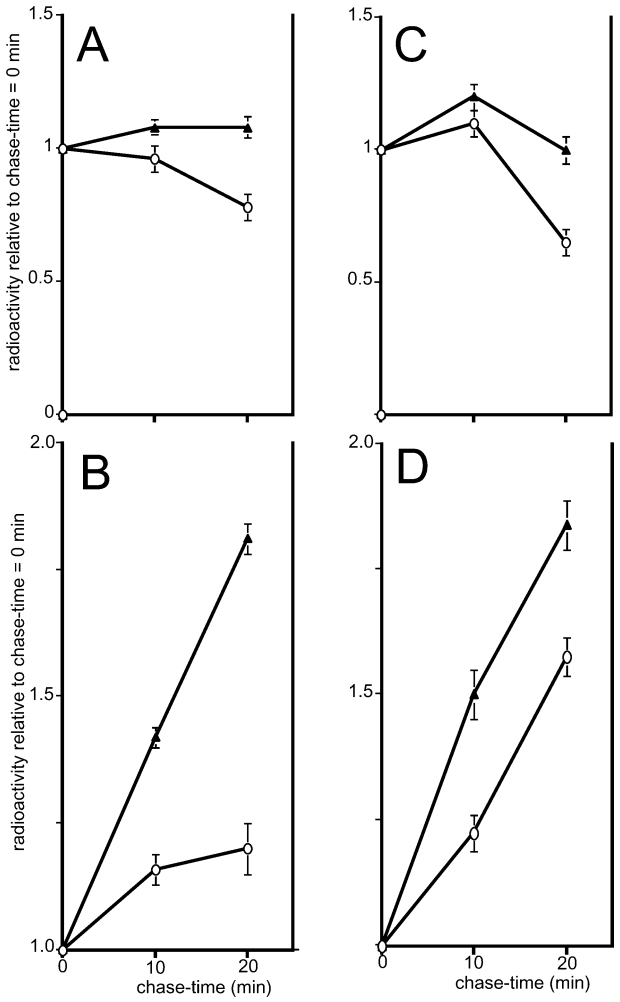

FIGURE 5: Continuous and pulse−chase labeling with [^{3}H]Man of glycolipid A and VSG in wild-type and *GPIdeAc* knockout trypanosomes. Wild-type (WT) and *GPIdeAc* knockout (KO) trypanosomes were pulse-labeled with [^{3}H]Man for 20 min followed by a chase with excess mannose (circles) or without a chase (triangles). Aliquots of labeled cells were recovered at 0, 10, and 20 min chase. Total GPI glycolipids were extracted and analyzed by HPTLC and phosphorimagery. The amount of radiolabel in glycolipid A was quantified, normalized to the 0 min chase value, and plotted as a function of time (panels A and C). Other aliquots from the same experiments were processed for SDS−PAGE, and the amount of [^{3}H]Man label in the VSG band was quantified, normalized to the 0 min chase value, and plotted as a function of time (panels B and D). The results show the means and standard errors of two separate experiments.

the ER) represents a 2.3-fold increase in lumenal glycolipid A in absolute terms when taking into account the 1.15-fold increase in total glycolipid A. These data are broadly consistent with the 2.8-fold increase in the rate of Gal-A synthesis, described above.

Taken together, these data suggest that the complex phenotype observed in the *GPIdeAc* knockout trypanosomes is due to a 2.3-fold increase in the steady-state levels of glycolipid A in the lumen of the ER compared with wild-type cells.

DISCUSSION

GPIdeAc shows significant homology with mammalian acyloxyacylhydrolases that degrade and detoxify bacterial lipid A in macrophage lysosomes (*67*−*70*). However, despite significant sequence and domain structure similarity, *T. brucei* GPIdeAc does not localize to the trypanosome lysosome, a discrete organelle between the nucleus and the flagellar pocket (*55*). Instead, immunostaining of overexpressed HA-tagged GPIdeAc produced a reticular perinuclear pattern similar and contiguous, but barely coincident, with the staining for the ER marker BiP (Figure 1). This staining pattern is clearly different from those for the Golgi apparatus, the mitochondrion, and the endosomal system of the parasite (*54*−*57*). We tentatively suggest that GPIdeAc may occupy a subcompartment of the ER dedicated to GPI biosynthesis that is devoid of other markers. A similar conclusion has been reached, on biochemical grounds, for components of the mammalian GPI pathway (*71*). A more detailed description of the location of GPIdeAc is beyond the scope of this paper.

The accumulation of glycolipid C′ in cell-free system experiments using *GPIdeAc* knockout trypanosome membranes suggests that the principal role of GPIdeAc is to convert glycolipid C′ to glycolipid A′ (*50*) (Figure 6). We postulate that deletion of GPIdeAc activity causes upregulation of a compensatory activity, called here GPI inositol deacylase-2 (GPIdeAc-2), that prevents GPI synthesis from stalling at glycolipid C′. The elevated levels of GPIdeAc-2 are further postulated to increase the level of lumenal glycolipid A (by shifting the A ↔ C equilibrium to the left), thus giving rise to increased synthesis of Gal-A GPI species. There are three galactosyltransferases (one βGal and two αGal transferases) that modify GPIs in the ER (*7*, *72*) and provide substrates for the addition of up to three further αGal residues in the Golgi apparatus (*73*).

The model satisfies the following facts and assumptions: (i) The upregulation of enzymes to compensate for gene deletions is known to occur in *T. brucei* (*74*). (ii) The active sites of the GlcNAc-transferase and GlcNAc-PI de-*N*-acetylase face the cytoplasm (*33*). (iii) The active sites of the Dol-P-Man-dependent MT-1 and MT-3 α-mannosyltransferases face the ER lumen (*39*). (iv) All mannosylated GPI intermediates (except glycolipid C) are found on both sides of the ER (*47*). (v) The acyl-CoA-independent inositol acyltransferase most likely faces the ER lumen (*50*, *75*). (vi) GPIdeAc faces the ER lumen (*50*). (vii) The acyl-CoA-dependent (*14*, *76*) and acyl-CoA binding protein (ACBP) stimulated (*77*) fatty acid remodeling machinery most likely faces the cytoplasm. (viii) Essentially all glycolipid C is in the lumen of the ER (*47*). (ix) Catabolism of GPI intermediates most likely proceeds primarily from glycolipid C (*78*). The model is also predicated on unidirectional transport of glycolipid θ and glycolipid A, whereas the earlier (non-ethanolamine phosphate-containing) species are assumed to undergo bidirectional movement. The unidirectional movement of glycolipid θ and glycolipid A (in a process that could, potentially, be coupled) might explain why glycolipid C (*47*) and Gal-A species (*79*) are found only in the lumen of the ER and would explain why the upregulation of GPIdeAc-2 would lead to an accumulation of glycolipid A specifically in the lumen of the ER.

The exit of non-protein-linked free GPIs from the ER and appearance on the exoplasmic leaflet of the plasma membrane have been demonstrated in mammalian cells (*80*−*82*), *Leishmania* promastigotes (*24*), and the procyclic form of *T. brucei* (*74*, *83*) but not previously in the bloodstream form

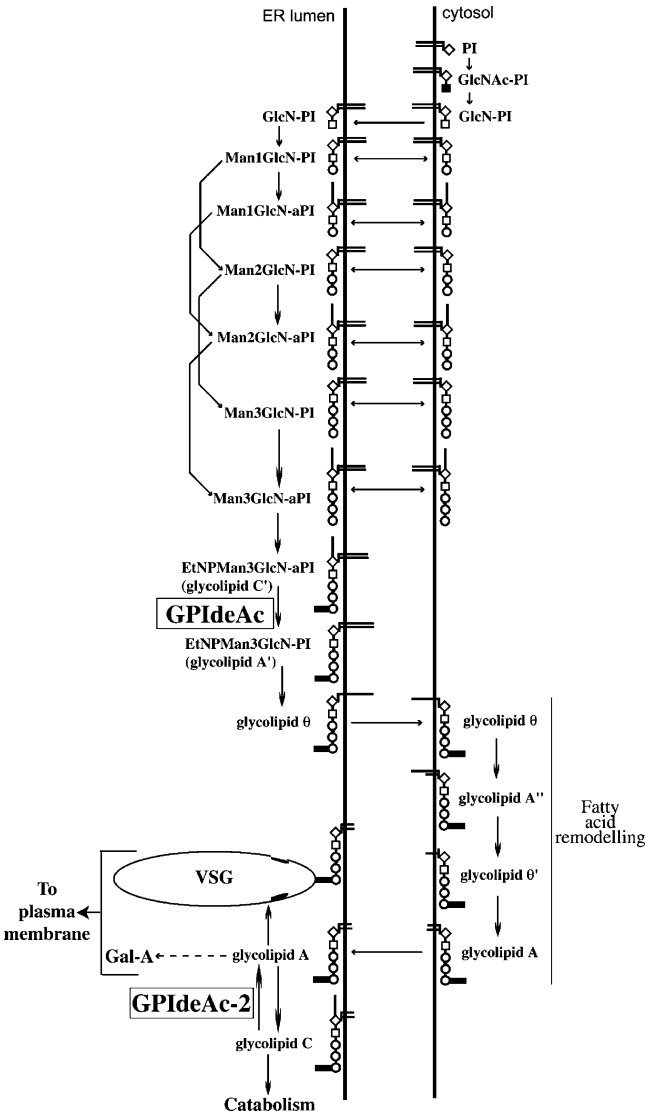

FIGURE 6: Proposed model for the biosynthesis of GPI precursors in the endoplasmic reticulum of bloodstream form of *T. brucei*. The basis of the model is described in the text. The enzymes GPIdeAc and GPIdeAc-2 are proposed to act primarily at the sites indicated in the model in wild-type cells. In the *GPIdeAc* null mutant, we suggest that upregulation of GPIdeAc-2 activity allows some of it to take the place of GPIdeAc for the conversion of glycolipid C′ to glycoloipid A′. Increased GPIdeAc-2 activity would also accelerate the conversion of glycolipid C to glycolipid A (the proposed site of GPIdeAc-2 action in wild-type cells) that manifests itself in the increased synthesis of Gal-A glycolipids and their export to the cell surface.

of *T. brucei*. The data in Figure 3 show clearly that glycolipid A and its galactosylated metabolites reach a GPI-PLC accessible location (most likely the plasma membrane) in the bloodstream form of parasites. Nevertheless, in wild-type parasites, the steady-state pool of glycolipid A is only 24000 copies per cell (*84*); cf. 5 million VSG dimers. Thus, the presence of even a large proportion of glycolipid A and Gal-A at the plasma membrane of wild-type cells is of dubious significance, unless they are concentrated into one region. More likely, the presence of free GPIs simply represents the exit of some lumenally disposed glycolipid A and Gal-A from the ER by bulk flow. The fact that the some of the glycolipid A is metabolized to fully galactosylated GPIs before reaching the plasma membrane suggests that the free GPIs travel by conventional means via the Golgi apparatus [where Gal_3-GPIs are processed to Gal_{4-6}-GPIs (*7*, *73*)].

In summary, we show here that the bloodstream form of *T. brucei* compensates for the loss of ER-resident GPIdeAc activity. The compensatory mechanism causes a change in the metabolism of GPI precursors in the parasite such that the rate of synthesis and steady-state levels of free galactosylated GPIs are increased about 3-fold. We also show that free GPI molecules reach the plasma membrane of the parasite and that the plasma membrane acts as a sink for excess free GPIs. Finally, we have shown that only about one-third of glycolipid A molecules are competent for transfer to nascent VSG molecules in wild-type trypanosomes and that deletion of the *GPIdeAc* gene increases the proportion of transfer-competent glycolipid A molecules. We postulate that the compensatory mechanism is the upregulation of a second (GPIdeAc-2) activity that restores the necessary flux through the GPI biosynthetic pathway but, in doing so, perturbs the pathway to give rise to the aforementioned effects. Consistent with this view, we have recently labeled membranes from *GPIdeAc* null mutant trypanosomes with [^{3}H]diisopropyl fluorophosphate and found a candidate for GPIdeAc-2. Future GPIdeAc-2 purification, cloning, and gene knockout studies should allow us to test these hypotheses.

ACKNOWLEDGMENT

We thank Anant Menon for helpful comments and Jay Bangs for anti-BiP antibodies.

REFERENCES

1. Ferguson, M. A. J. (1999) *J. Cell Sci. 112*, 2799−2808.
2. Morita, Y. S., Acosta-Serrano, A., and Englund P. T. (2000) in *Oligosaccharides in Chemistry and Biology—A Comprehensive Handbook* (Sinay, E. P., and Hart, G. W., Eds.) pp 417−433, Wiley-VCH, Weinheim, Germany.
3. Kinoshita, T., and Inoue, N. (2000) *Curr. Opin. Chem. Biol. 4*, 632−638.
4. McConville, M. J., Mullin, K. A., Ilgoutz, S. C., and Teasdale, R. D. (2002) *Microbiol. Mol. Biol. Rev. 66*, 122−154.
5. Ferguson, M. A. J., Brimacombe, J. S., Brown, J. R., Crossman, A., Dix, A., Field, R. A., Güther, M. L. S., Milne, K. G., Sharma, D. K., and Smith, T. K. (1999) *Biochim. Biophys. Acta 1455*, 327−340.
6. Ferguson, M. A. J., Homans, S. W., Dwek, R. A., and Rademacher, T. W. (1988) *Science 239*, 753−759.
7. Mehlert, A., Richardson, J. M., and Ferguson, M. A. (1998) *J. Mol. Biol. 277*, 379−392.
8. Cross, G. A. M. (1996) *BioEssays 18*, 283−291.
9. Steverding, D., Stierhof, Y. D., Fuchs, H., Tauber, R., and Overath, P. (1995) *J. Cell Biol. 131*, 1173−1182.
10. Steverding, D. (2000) *Parasitol. Int. 48*, 191−198.
11. Nagamune, K., Nozaki, T., Maeda, Y., Ohishi, K., Fukuma, T., Hara, T., Schwarz, R. T., Sutterlin, C., Brun, R., Riezman, H., and Kinoshita, T. (2000) *Proc. Natl. Acad. Sci. U.S.A. 97*, 10336−10341.
12. Chang, T., Milne, K. G., Güther, M. L. S., Smith, T. K., and Ferguson, M. A. J. (2002) *J. Biol. Chem. 277*, 50176−50182.
13. Masterson, W. J., Doering, T. L., Hart, G. W., and Englund, P. T. (1989) *Cell 56*, 793−800.
14. Masterson, W. J., Raper, J., Doering, T. L., Hart, G. W., and Englund, P. T. (1990) *Cell 62*, 73−80.
15. Menon, A. K., Schwarz, R. T., Mayor, S., and Cross, G. A. M. (1990) *J. Biol. Chem. 265*, 9033−9042.
16. Menon, A. K., Mayor, S., and Schwarz, R. T. (1990) *EMBO J. 9*, 4249−4258.
17. Güther, M. L. S., and Ferguson, M. A. J. (1995) *EMBO J. 14*, 3080−3093.

18. Morita, Y. S., Acosta-Serrano, A., Buxbaum, L. U., and Englund, P. T. (2000) *J. Biol. Chem. 275*, 14147−14154.
19. Heise, N., Raper, J., Buxbaum, L. U., Peranovich, T. M., and de Almeida, M. L. (1996) *J. Biol. Chem. 271*, 16877−16887.
20. Striepen, B., Dubremetz, J.-F., and Schwarz, R. T. (1999) *Biochemistry 38*, 1478−1487.
21. Gerold, P., Jung, N., Azzouz, N., Freiberg, N., Kobe, S., and Schwarz, R. T. (1999) *Biochem. J. 344*, 731−738.
22. Smith, T. K., Milne, F. C., Sharma, D. K., Crossman, A., Brimacombe, J. S., and Ferguson, M. A. J. (1997) *Biochem. J. 326*, 393−400.
23. Ralton, J. E., and McConville, M. J. (1998) *J. Biol. Chem. 273*, 4245−4257.
24. Ralton, J. E., Mullin, K. A., and McConville, M. J. (2002) *Biochem. J. 363*, 365−375.
25. Sutterlin, C., Escribano, M. V., Gerold, P., Maeda, Y., Mazon, M. J., Kinoshita, T., Schwarz, R. T., and Riezman, H. (1998) *Biochem. J. 332*, 153−159.
26. Flury, I., Benachour, A., and Conzelmann, A. (2000) *J. Biol. Chem. 275*, 24458−24465.
27. Grimme, S. J., Westfall, B. A., Wiedman, J. M., Taron, C. H., and Orlean, P. (2001) *J. Biol. Chem. 276*, 27731−27739.
28. Franzot, S. P., and Doering, T. L. (1999) *Biochem. J. 340*, 25−32.
29. Hirose, S., Prince, G. M., Sevlever, D., Ravi, L., Rosenberry, T. L., Ueda, E., and Medof, M. E. (1992) *J. Biol. Chem. 267*, 16968−16974.
30. Puoti, A., and Conzelmann, A. (1993) *J. Biol. Chem. 268*, 7215−7224.
31. Chen, R., Walter, E. I., Parker, G., Lapurga, J. P., Millan, J. L., Ikehara, Y., Udenfriend, S., and Medof, M. E. (1998) *Proc. Natl. Acad. Sci. U.S.A. 95*, 9512−9517.
32. Watanabe, R., Murakami, Y., Marmor, M. D., Inoue, N., Maeda, Y., Hino, J., Kangawa, K., Julius, M., and Kinoshita, T. (2000) *EMBO J. 19*, 4402−4411.
33. Vidugiriene, J., and Menon, A. K. (1993) *J. Cell Biol. 121*, 987−996.
34. Doerrler, W. T., Ye, J., Falck, J. R., and Lehrman, M. A. (1996) *J. Biol. Chem. 271*, 27031−27038.
35. Morita, Y. S., and Englund, P. T. (2001) *Mol. Biochem. Parasitol. 115*, 157−164.
36. Smith, T. K., Cottaz, S., Brimacombe, J. S., and Ferguson, M. A. J. (1996) *J. Biol. Chem. 271*, 6476−6482.
37. Smith, T. K., Sharma, D. K., Crossman, A., Dix, A., Brimacombe, J. S., and Ferguson, M. A. J. (1997) *EMBO J. 16*, 6667−6675.
38. Smith, T. K., Sharma, D. K., Crossman, A., Brimacombe, J. S., and Ferguson, M. A. (1999) *EMBO J. 18*, 5922−5930.
39. Maeda, Y., Watanabe, R., Harris, C. L., Hong, Y., Ohishi, K., Kinoshita, K., and Kinoshita, T. (2001) *EMBO J. 20*, 250−261.
40. Takahashi, M., Inoue, N., Ohishi, K., Maeda, Y., Nakamura, N., Endo, Y., Fujita, T., Takeda, J., and Kinoshita, T. (1996) *EMBO J. 15*, 4254−4261.
41. Sutterlin, C., Escribano, M. V., Gerold, P., Maeda, Y., Mazon, M. J., Kinoshita, T., Schwarz, R. T., and Riezman, H. (1998) *Biochem. J. 332*, 153−159.
42. Flury, I., Benachour, A., and Conzelmann, A. (2000) *J. Biol. Chem. 275*, 24458−24465.
43. Hong, Y., Maeda, Y., Watanabe, R., Inoue, N., Ohishi, K., and Kinoshita, T. (2000) *J. Biol. Chem. 275*, 20911−20919.
44. Taron, C. H., Wiedman, J. M., Grimme, S. J., and Orlean, P. (2000) *Mol. Biol. Cell 11*, 1611−1630.
45. Fraering, P., Imhof, I., Meyer, U., Strub, J. M., van-Dorsselaer, A., Vionnet, C., and Conzelmann, A. (2001) *Mol. Biol. Cell 12*, 3295−306.
46. Ohishi, K., Inoue, N., and Kinoshita, T. (2001) *EMBO J. 20*, 4088−4098.
47. Vidugiriene, J., and Menon, A. K. (1994) *J. Cell Biol. 127*, 333−341.
48. Murakami, Y., Siripanyapinyo, U., Hong, Y., Kang, J. Y., Ishihara, S., Nakakuma, H., Maeda, Y., and Kinoshita, T. (2003) *Mol. Biol. Cell 10* (in press).
49. Umemura, M., Okamoto, M., Nakayama, K., Sagane, K., Tsukahara, K., Hata, K., and Jigami, Y. (2003) *J. Biol. Chem. 278*, 23639−23647.
50. Güther, M. L. S., Leal, S., Morrice, N., Cross, G. A. M., and Ferguson, M. A. J. (2001) *EMBO J. 20*, 4923−4934.
51. Guther, M. L. S., Masterson, W. J., and Ferguson, M. A. J. (1994) *J. Biol. Chem. 269*, 18694−18701.
52. Ferguson, M. A. J. (1992) in *Lipid Modification of Proteins: a Practical Approach* (Turner, A. J., and Hooper, N., Eds.) pp 191−230, IRL Press, Oxford.
53. Schneider, P., and Ferguson, M. A. J. (1995) *Methods Enzymol. 250*, 614−630.
54. Pal, A., Hall, B. S., Nesbeth, D. N., Field, H. I., and Field, M. C. (2002) *J. Biol. Chem. 277*, 9529−9539.
55. Alexander, D. L., Schwartz, K. J., Balber, A. E., and Bangs, J. D. (2002) *J. Cell Sci. 115*, 3253−3263.
56. Grunfelder, C. G., Engstler, M., Weise, F., Schwarz, H., Stierhof, Y. D., Morgan, G. W., Field, M. C., and Overath, P. (2003) *Mol. Biol. Cell 14*, 2029−2040.
57. Vassella, E., Straesser, K., and Boshart, M. (1997) *Mol. Biochem. Parasitol. 90*, 381−385.
58. Bangs, J. D., Uyetake, L., Brickman, M. J., Balber, A. E., and Boothroyd, J. C. (1993) *J. Cell Sci. 105*, 1101−1113.
59. Cardoso de Almeida, M. L., and Turner, M. J. (1983) *Nature 302*, 349−352.
60. Ferguson, M. A. J., Haldar, K., and Cross, G. A. M. (1985) *J. Biol. Chem. 260*, 4963−4968.
61. Bangs, J. D., Andrews, N. W., Hart, G. W., and Englund, P. T. (1986) *J. Cell Biol. 103*, 255−263.
62. Ferguson, M. A. J., Duszenko, M., Lamont, G., Overath, P., and Cross, G. A. M. (1986) *J. Biol. Chem. 261*, 356−362.
63. Bohme, U., and Cross, G. A. (2002) *J. Cell Sci. 115*, 805−816.
64. Güther, M. L., Treumann, A., and Ferguson, M. A. (1996) *Mol. Biochem. Parasitol. 77*, 137−145.
65. Masterson, W. J., and Ferguson, M. A. J. (1991) *EMBO J. 10*, 2041−2045.
66. Ralton, J. E., Milne, K. G., Güther, M. L. S., Field, R. A., and Ferguson, M. A. J. (1993) *J. Biol. Chem. 268*, 24183−24189.
67. Munford, R. S., and Hall, C. L. (1986) *Science 234*, 203−205.
68. Munford, R. S., and Hall, C. L. (1989) *J. Biol. Chem. 264*, 15613−15619.
69. Munford, R. S., and Hunter, J. P. (1992) *J. Biol. Chem. 267*, 10116−10121.
70. Staab, J. F., Ginkel, D. L., Rosenberg, G. B., and Munford, R. S. (1994) *J. Biol. Chem. 269*, 23736−23742.
71. Vidugiriene, J., Sharma, D. K., Smith, T. K., Baumann, N. A., and Menon, A. K. (1999) *J. Biol. Chem. 274*, 15203−15212.
72. Mayor, S., Menon, A. K., and Cross, G. A. M. (1992) *J. Biol. Chem. 267*, 754−761.
73. Bangs, J. D., Doering, T. L., Englund, P. T., and Hart, G. W. (1988) *J. Biol. Chem. 263*, 17697−17705.
74. Vassella, E., Bütikofer, P., Engstler, M., Jelk, J., and Roditi, I. (2003) *Mol. Biol. Cell 14*, 1308−1318.
75. Smith, T. K., Crossman, A., Paterson, M. J., Borissow, C. N., Brimacombe, J. S., and Ferguson, M. A. (2002) *J. Biol. Chem. 277*, 37147−37153.
76. Paul, K. S., Jiang, D., Morita, Y. S., and Englund, P. T. (2001) *Trends Parasitol. 17*, 381−387.
77. Milne, K. G., and Ferguson, M. A. (2000) *J. Biol. Chem. 275*, 12503−12508.
78. Milne, K. G., Ferguson, M. A., and Englund, P. T. (1999) *J. Biol. Chem. 274*, 1465−1471.
79. McConville, M. J., and Menon, A. K. (2000) *Mol. Membr. Biol. 17*, 1−16.
80. van't Hof, W., Rodriguez-Boulan, E., and Menon, A. K. (1995) *J. Biol. Chem. 270*, 24150−24155.
81. Singh, N., Liang, L. N., Tykocinski, M. L., and Tartakoff, A. M. (1996) *J. Biol. Chem. 271*, 12879−12884.
82. Baumann, N. A., Vidugiriene, J., Machamer, C. E., and Menon, A. K. (2000) *J. Biol. Chem. 275*, 7378−7389.
83. Lillico, S., Field, M. C., Blundell, P., Coombs, G. H., and Mottram, J. C. (2003) *Mol. Biol. Cell 14*, 1182−1194.
84. Doering, T. L., Pessin, M. S., Hart, G. W., Raben, D. M., and Englund, P. T. (1994) *Biochem. J. 299*, 741−746.

BI034869G